

# Trilevel Neural Architecture Search for Efficient Single Image Super-Resolution

Yan Wu<sup>1</sup>, Zhiwu Huang<sup>1</sup>, Suryansh Kumar<sup>1</sup>, Rhea Sanjay Sukthanker<sup>1</sup>, Radu Timofte<sup>1</sup>, Luc Van Gool<sup>1,2</sup>

<sup>1</sup>Computer Vision Lab, ETH Zürich, Switzerland

<sup>2</sup>VISICS, KU Leuven, Belgium

wuyan@student.ethz.ch, rhea.sukthanker@inf.ethz.ch,

{zhiwu.huang, sukumar, radu.timofte, vangool}@vision.ee.ethz.ch

## Abstract

This paper proposes a trilevel neural architecture search (NAS) method for efficient single image super-resolution (SR). For that, we first define the discrete search space at three-level, i.e., at network-level, cell-level, and kernel-level (convolution-kernel). For modeling the discrete search space, we apply a new continuous relaxation on the discrete search spaces to build a hierarchical mixture of network-path, cell-operations, and kernel-width. Later an efficient search algorithm is proposed to perform optimization in a hierarchical supernet manner that provides a globally optimized and compressed network via joint convolution kernel width pruning, cell structure search, and network path optimization. Unlike current NAS methods, we exploit a sorted sparsestmax activation to let the three-level neural structures contribute sparsely. Consequently, our NAS optimization progressively converges to those neural structures with dominant contributions to the supernet. Additionally, our proposed optimization construction enables a simultaneous search and training in a single phase, which dramatically reduces search and train time compared to the traditional NAS algorithms. Experiments on the standard benchmark datasets demonstrate that our NAS algorithm provides SR models that are significantly lighter in terms of the number of parameters and FLOPS with PSNR value comparable to the current state-of-the-art.

## 1. Introduction

Image super-resolution (SR) aims to enhance the resolution of a given image from low-resolution to high-resolution. It is well-known that image SR is an ill-posed problem, and lately, many deep learning-based methods have emerged to address it [6, 13, 30, 5, 29, 18, 15]. These methods generally have a set of neural computation blocks like residual blocks to better encode input images and a few upsampling layers to enhance spatial resolution. To further increase efficiency and performance of the designed

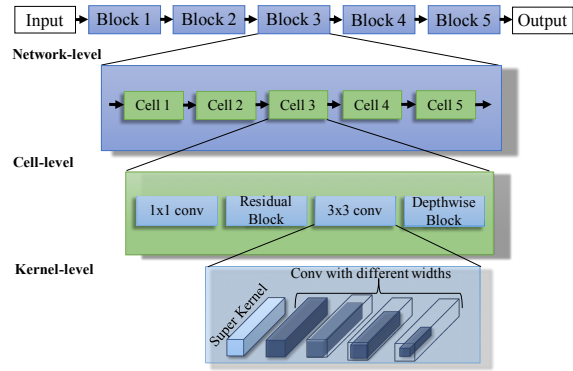


Figure 1: A typical trilevel neural architecture design for image SR.

SR network, as illustrated in Fig.(1), the conventional deep SR methods typically opt for the following variations on the trilevel neural architecture design: (a) A *network-level* optimization to properly position the upsampling layers [19, 12]. (b) A *cell-level* optimization to improve the capacities of encoding or upscaling [20, 4]. (c) A *kernel-level* optimization to make a trade-off between an operator’s capacity and its width (i.e., the number of input/output channels) for a compressed model [17, 7]. However, manually performing these optimizations for a favorable deep SR model requires a lot of time, effort, and domain expertise. Further, handcrafted architectures are often not optimal and may be computationally inefficient for real-world applications.

To overcome the above shortcomings, this paper proposes to automate the whole trilevel neural architectures’ design for efficient image SR. For that, we first suggest a comprehensive search space defined at three different levels (see Fig.1). Concretely, our network-level search space is composed of all the candidate network paths. Whereas, cell-level search space contains a mixture of all possible candidate operations, and the kernel-level search space is a single convolutional kernel with a defined subset of the kernel-width dimension §3. Since these designated search spaces are discrete, we perform a continuous relaxation of these search spaces to be optimized efficiently in a differen-

tiable manner. We follow DARTS [20] and AGD [7] to employ supercell and superkernel continuous relaxation modeling strategies to model kernel-level and cell-level search spaces, respectively. Yet, continuous modeling of network-level search space is a non-trivial task. One way to solve that is to adopt the trellis-like supernet from Auto-DeepLab [19], which combines all the possible paths in a compact network and finally selects the optimal path with maximum probability. However, in the trellis-supernet, any possible path’s information flow is highly-entangled within the trellis, and thus the derived path and cell architectures may not be optimal. Also, the length of the path we get from a trellis-like supernet is fixed. Hence, we strive for a network search modeling with relaxed disentangled network paths, where distinct paths contribute independently to the supernet such that the flow of the network paths becomes more flexible. To that end, we introduce a tree-like supernet modeling where paths are enumerated independently and are pruned once it makes reasonable contributions to the supernet (see Fig.1). Our tree-like supernet disentangles the sequential network path dependency and gives a better trade-off between memory consumption and cell sharing across layers.

Finally, we perform a new continuous relaxation of the designed trilevel representations *i.e.*, supernet, supercell, and superkernel representation, for an enlarged search space. The enlarged search space allows us to perform a differentiable architecture search with gradient descent optimization to obtain an optimal supernet. The standard continuous relaxation uses softmax [20], which fails to produce sparse distribution. Hence, it struggles to seek the most dominant operation selected for an optimal architecture design. In that case, the softmax usage is likely to prevent the supernet from converging to a dominant candidate architecture. Therefore, we adhere to exploit a sparsestmax strategy for the continuous relaxation of our suggested trilevel search space. Sparsestmax generate sparse distribution [25] while preserving most of the attractive properties of softmax (*e.g.*, differentiability and convexity). Nevertheless, the sparsestmax is still not aligned well with our sequential setup on the network-level search space. So, we use a sorted sparsestmax, where the network level path sparsity is arranged in descending order, which helps us prune the tail of the network path for significant model compression. We observed that sparsestmax generally gives excellent sparsity, *i.e.*, a minimal number of candidates makes non-zero contributions to the supernet, such that it can be directly selected for the design of optimal architecture. Besides that, it enables us to go for a new NAS training scheme, where the training can be done from search rather than from scratch which is widely practiced by traditional NAS algorithms.

We report our results on two popular SR benchmarks, *i.e.*, Set5 [1] and Set14 [31], as well as on the recent challenge benchmark [33]. Our best model is much lighter with

performance as good as the recent state-of-the-art methods. To sum up, our paper makes the following contribution to NAS and image SR:

- We propose a NAS algorithm to simultaneously search our defined trilevel search space for an efficient image SR architecture design. For the continuous relaxation of the enlarged trilevel search space, we introduce a new three-level hierarchical supernet modeling.
- For the optimization of relaxed trilevel search space, we exploit a ordered sparsestmax that has excellent capacity to provide sparse distribution on candidate architectures. Our new change to NAS enables us to blur the discrepancy between the search and training phase, resulting in single phase continuous learning which leads to considerable training time reduction.
- SR model obtained by our proposed NAS is much lighter with PSNR value close to the best available methods.

## 2. Relevant Work

Several solutions to a single image super-resolution problem based on one-level and bi-level NAS core have appeared recently. Popular one-level NAS like the evolutionary algorithms (*e.g.*, [23, 24]), and the reinforcement learning-based NAS methods (*e.g.*, [34, 35]) introduced input/output channel numbers into their search space for optimization. Recently, Zhang *et al.* [32] suggested a differentiable width-level architecture search method. They aim to select an optimal policy by keeping the same kernel-width, half the kernel-width, and double the kernel-width at each layer. However, based on the supernet design of [32], the search cost can dramatically increase if the kernel-width search space is further enlarged. Other variants of one-level NAS is Liu *et al.* [20] cell-level NAS. They proposed to model the basic cell of the network with a directed acyclic graph (DAG). It further relaxed the discrete search space into a continuous one via a softmax combination of all candidate operations on each edge, which constitute a supernet. This continuous relaxation enables a differentiable optimization of the supernet. Though being effective, it typically suffers from problems such as a large gap between the supernet and stand-alone architecture [3], aggregation of skip-connections [4] and large memory consumption [2].

Under bi-level NAS core, Stamoulis *et al.* [27] encoded candidate cell-level operations and kernel-level expansions into a single superkernel for each layer of the one-shot NAS supernet. This encoding reduces the NAS problem to finding the subset of kernel weights in each ConvNet layer. Fu *et al.* [7] proposed AGD, a differentiable NAS method to compress GAN based SR generator. Instead of searching for GAN architecture from scratch as done in [10, 9], AGD [7] leverage knowledge from the pre-trained SR models via knowledge distillation. Using knowledge distillation, they apply a differentiable NAS framework [20] to

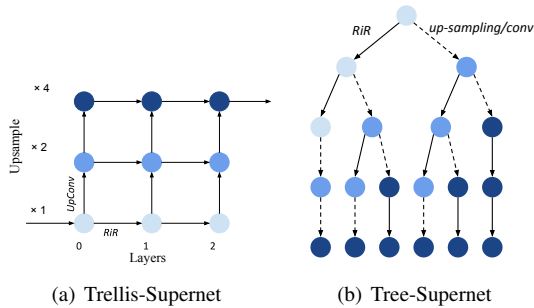


Figure 2: *Left*: Trellis-supernet modeling with 2 RiR and 2 Upsampling blocks. Vertical and horizontal axes show upsampling scale and layer number, respectively. Each intermediate feature map (blue node) has two paths to traverse: horizontal path (RiR block) and vertical path ( $\times 2$  Upsampling layer). The feature maps achieve the same scale when the same layer merged together. A feasible path traverse from the start of the node to the end node; *Right*: Tree-supernet modeling with 2 RiR and 2 Upsampling /Conv layers. Like Trellis-supernet, each intermediate feature map has 2 paths to travel. Here, each path is independent and do not merge, and any path starting from the root can be a feasible path.

search for each cell’s optimal operation (referred as cell-level architecture search) and pruning of the input/output channels for each operation (*i.e.*, kernel-level architecture search). However, AGD [7] overlooked the network-level search and kept the upsampling operations fixed at the network header part. Though the post-upsampling network design can be more efficient, lack of network-level optimization might have constrained the AGD performance. On contrary, Auto-DeepLab [19] proposes searching the network level structure along with the cell-level structure, which forms a hierarchical architecture search space. Concretely, it modeled the network-level search with one trellis-like supernet, where nodes represent the intermediate feature maps, and arrows between nodes indicate the corresponding cells. The trellis-like design allow the method to explore for a general network-level search space. Similarly, Guo *et al.* [12] used hierarchical NAS framework for SR problem [19]. The notable difference is that it leverages reinforcement learning for the cell-level and network-level architecture design. Exploring network-level design can be beneficial to the SR model. However, this work do not strive for kernel width pruning. Besides, the usage of reinforcement learning-based NAS introduces practical challenges.

### 3. Trilevel Architecture Search Space

To achieve the right balance between the model capacity and the model size with minimal loss in accuracy, we propose to search at kernel-level, cell-level, and network-level structures to get efficient SR network architecture. We exploit a novel structure for the network-level search space where all candidate network paths are enumerated in a tree structure. For the cell-level and kernel-level search space,

we leverage DARTS [20] and AGD [7] methodology. In the following subsections, we describe them accordingly.

#### 3.1. Network Level Search Space

Following AGD [7] and SRResNet [14], we define our network-level search space. The reason for that is their supernet architecture choice makes most of the computation in low-resolution feature space to gain computational efficiency. By fixing our supernet’s stem, which consumes marginal computation, we focus on searching the path of the remaining five residual blocks and two upsampling blocks. We replace the dense blocks in residual-in-residual (RiR) modules with five sequential layers containing searchable cell-level operators and kernel-level widths. For efficient upsampling block design, we replace the two originally designed upsampling blocks [7]. Instead, we include one PixelShuffle block, which contains a convolution layer (with an output channel number being  $n \times n \times 3$ ) [33], and a PixelShuffle layer to reach the target resolution with an upscaling factor of  $n$ . As the PixelShuffle block is fixed at the tail of the network [33], we add two regular convolution layers into the network-level search space so that we focus only on stacked five RiR blocks and two standard convolution layers for network path search.

To model the network-level search space, adopting the trellis-like structure from AutoDeep-Lab [19] seems like a feasible solution. However, as shown in Fig.2 (a), the trellis modeling aims to traverse all the sequential paths of the network blocks. Here, each path starts from the first node, representing the input feature map, and goes along a set of arrows to the target. Clearly, all the paths share most of the nodes and arrows. Such redundant sharing leads to extreme dependence among the paths, the cells, and the kernels as the paths hierarchically include them. Although the strong architecture sharing strategy saves a lot of training memory, it greatly limits the search space. Further, the tight entanglement is likely to harm the learning on each path’s contribution and the pruning of some redundant paths.

We propose a tree structure for a flexible network-level path search modeling to overcome the drawbacks mentioned above. As illustrated in Fig.2 (b), the tree modeling aims to traverse all the tree structure paths. Here, each node is merely connected to its father (if applicable) and children, and therefore, the dependency is highly relaxed. Nonetheless, we must maintain the associations at train time for lower memory consumption. Relaxing the correlations of different paths enables a flexible network-level search space. The lower dependency on paths may lead to a reliable association among cells and kernels due to their hierarchical connection, making their search spaces more general. Moreover, the introduced tree modeling enables better disentanglement among the paths allowing us to perform pruning on a redundant path. Also, it support the removal

of the candidate paths once they contribute to the supernet.

### 3.2. Cell Level and Kernel Level Search Space

To define the search space at kernel-level and cell-level, we followed AGD work [7]. At cell-level, we search for five RiR blocks with each block containing five searchable cells, *i.e.*, in total, 25 searchable cells. For each cell, we select one of the following candidate operations:

- (i) Conv  $1 \times 1$ , (ii) Residual Block (2 layers of Conv  $3 \times 3$  with a skip-connection), (iii) Conv  $3 \times 3$ , (iv) Depthwise Block (Conv  $1 \times 1$  + Depthwise Conv  $3 \times 3$  + Conv  $1 \times 1$ ).

For kernel-level search, we follow [7] *superkernel* framework to model this search space. For each convolution kernel, we set up a superkernel which has the full channels. To prune the channel number of the superkernel, a set of searchable expansion ratios  $\phi = [\frac{1}{3}, \frac{1}{2}, \frac{4}{5}, \frac{5}{6}, 1]$  is defined, and parameters  $\gamma_i$  which indicates the probability to choose the  $i$ -th expansion ratio is to be optimized.

## 4. Proposed Method

We propose a differentiable NAS algorithm that utilizes the suggested continuous relaxation of discrete trilevel search space §3. The key idea is to relax the discrete trilevel search space’s explicit selection to an implicit selection from a hierarchical mixture of all the involved candidates in the search space. The continuous relaxation enables us to select the candidate with the highest contribution to the supernet in a fully-differentiable manner. Subsequently, the whole supernet can be optimized to achieve an efficient architecture. One of the popular continuous relaxation strategies is to apply softmax to achieve a mixture of all candidate network operations. However, softmax cannot produce sparse distribution, and thus, it fails to reflect the dominant operation, which can be vital for an efficient architecture design. So, the usage of softmax can prevent the supernet from converging to a dominant candidate architecture. To address this issue, we propose sparsestmax, which produces good sparsity over the continuous relaxation and can seek dominant candidate architectures while having properties such as convexity and differentiability like softmax.

Further, the suggested trilevel search space modeling facilitates the pruning of the paths, as discussed before. To prune the paths better, we additionally introduce a novel ordering constraint to the sparsestmax. Ordering constraint makes the candidate paths to have heavier heads (*i.e.*, with more dominant contributions to the path) and lighter tails (*i.e.*, with marginal contributions to the path) so that tails can be easily removed. Consequently, our supernet generally converges to a reasonably sparse network due to the usage of ordered sparsestmax on the mixture of all candidate networks. As a benefit, the candidate architecture given by the sparsestmax activation is selected directly to design the optimal architecture. We observed that we get a

marginal difference between the searched architecture and trained architecture, which provides an added advantage, *i.e.*, we can start training the network from the parameters learned during the search phase rather than from scratch.

### 4.1. Sorted Sparsestmax Supernet

To achieve a continuous relaxation of the discrete network-level search space, we suggest aggregating all the network paths with a set of continuous combination weights to constitute a supernet. This reduces the task of architecture search to learning the set of continuous variables and their intrinsic network parameters, and thus, the whole supernet can be optimized in a differentiable manner using gradient descent algorithms. In our introduced network backbone §3, since the upsampling layer is out of the network-level search space, each feature map (*i.e.*, node) in the tree model can be used as the output of its corresponding path, and then the output can be fed into the upsampling layer to get the desired resolution. Hence, the aggregation over all the paths is reduced to the fusion over all the involved feature maps. In particular, we define a set of contribution weights  $\beta$  for all the feature maps from the involved network paths based on our suggested tree model (Fig.2), and the output of the supernet is therefore a weighted combination of all the intermediate features maps. Given a tree model of the network-level search space with  $N$  paths being  $P = \{P_1, \dots, P_N\}$  where  $P_i$  has  $M_i$  feature maps, the output of the whole supernet (*i.e.*, the mixture of all the candidate paths) is defined as:

$$O_{tree} = \sum_{i=0}^N \sum_{j=0}^{M_i} F_N(\beta_{i,j}; \beta) f_{i,j}, \quad (1)$$

where  $f_{i,j}$  is the feature map at the  $j$ -th layer of  $P_i$ , and  $F_N(\beta_{i,j}; \beta)$  indicates the normalized combination weight over the feature map  $f_{i,j}$

We could follow differentiable NAS like [20, 7, 19] and apply  $\text{softmax}(\beta)$  to normalize the combination weights which reflect the contribution of the candidates to the mixture. However, softmax generally produces non-zero parameters *i.e.* smoothly varying parameters. Hence, the candidate contributions is comparatively uniform, that is inferior in sparsity, which prevents the supernet from converging to a dominant candidate architecture. To address this issue, we use sparsestmax [26] that produce sparse distributions while maintaining some useful properties of softmax:

$$F_N(\beta, r) := \underset{\mathbf{q} \in \Delta_r^{k-1}}{\text{argmin}} \|\mathbf{q} - \beta\|_2^2, \quad (2)$$

where  $\Delta_r^{k-1} := \{\mathbf{q} \in \mathbb{R}^K | \mathbf{1}^T \mathbf{q} = 1, \|\mathbf{q} - \mathbf{u}\|_2 \geq r, \mathbf{q} \geq \mathbf{0}\}$  indicates a simplex with a circular constraint  $\mathbf{1}^T \mathbf{q} = 1, \|\mathbf{q} - \mathbf{u}\|_2 \geq r, \mathbf{u} = \frac{1}{K} \mathbf{1}$  is the center of the simplex,  $\mathbf{1}$  is a vector of ones, and  $r$  is radius of the circle. The basic idea



of sparsestmax is that it returns the Euclidean projection of the input vector  $\beta$  onto the probability simplex. This projection is likely to touch the simplex boundary, in which case sparsestmax produces sparse distributions. To achieve a better sparsity, sparsestmax further introduces a circular constraint that enables a progressive production of sparsity by linearly increasing  $r$  from zero to  $r_c$ , where  $r_c$  is the radius of the circumcircle of the simplex. For detailed evaluations on the superiority of sparsestmax over softmax as well as sparsemax [21, 22], we refer readers to [26].

While sparsestmax gives sparse distributions, it is not aligned well with our sequential setup. Concretely, given a path,  $P_i$  that consists of  $M_i$  nodes (*i.e.*, feature maps), the direct use of sparsestmax may produce unordered non-zero combination weights on the nodes (the extreme case is all of them distribute at the odd/even nodes). In that case, we cannot prune the path well unless the sparsity is ordered. In other words, as long as the non-zero combination weights are descending along the path so that all the zero weights appear at the tail of the path, we can perform network-level pruning. This motivate us to exploit a sorted sparsestmax. Hence, we further impose an ordering constraint to the weights  $\beta_i$  within each path  $p_i$ . Intuitively, this helps the output feature maps from shallower layers to share more contributions to the supernet. Thus, we formulated **sorted sparsestmax** as

$$F_N(\beta, r) := \operatorname{argmin}_{q \in \Delta_r^{k-1}} \|q - \beta\|_2^2 + \lambda \sum_i \sum_j (\beta_{i,j} - \beta_{i,j-1}) \quad (3)$$

here  $\lambda$  is a trade-off constant.

Now, for its usage in our method, we apply sparsestmax directly to relax the discrete search space into a continuous one (since the cell-level network has no sequential properties). Notably, we define a set of operations' contribution weights  $\alpha$ , such that the output is a normalized weighted combination of all the candidate operations. For our task, the output of  $i^{\text{th}}$  cell  $C_i$  is the weighted sum of all the 4 features maps from the 4 candidate operations, *i.e.*,

$$C_i = \sum_{o \in O} F_N(\alpha_i^{(o)}; \alpha_i) o(C_{i-1}) \quad (4)$$

where  $F_N$  corresponds to sparsestmax,  $o(C_{i-1})$  is one operations selected from the cell-level space  $O$  over  $C_{i-1}$ .

For the continuous relaxation of the kernel-level search space, one solution is to apply sparsestmax to combine all the involved kernels' expansions. However, as the number of kernels is huge, and each one can have many different expansions, it leads to exponentially possible combinations. It is non-trivial to create a set of independent convolutional kernels with various widths for each candidate operator. So, we leave this direction to future work. We apply the differentiable Gumbel-softmax sampling to keep the setup consistent with AGD [7]. As for optimizing expansion ratio

---

### Algorithm 1: The Proposed TrileveNAS

---

- 1: **Input:** dataset  $\chi = \{x_i\}_{i=1}^N$ , pretrained generator  $G_0$ , search space and supernet  $G$ , epochs to pretrain ( $T_1$ ), search ( $T_2$ ) and train-from-scratch ( $T_3$ )
  - 2: **Output:** trained efficient generator  $G^*$
  - 3: Equally split  $\chi$  into  $\chi_1$  and  $\chi_2$  and initialize supernet weight  $w$  and architecture parameters  $\{\alpha, \beta, \gamma\}$  with uniform distribution
  - 4: **# First Step: Pretrain**
  - 5: **for**  $t \leftarrow 1$  to  $T_1$  **do**
  - 6:   Get a batch of data  $X_1$  from  $\chi_1$
  - 7:   **for**  $\gamma$  in  $[\gamma_{\max}, \gamma_{\min}, \gamma_{\text{random1}}, \gamma_{\text{random2}}]$  **do**
  - 8:      $g_w^{(t)} = \nabla_w d(G(X_1, \alpha, \beta, \gamma), G_0(X_1))$
  - 9:      $w^{(t+1)} = \text{update}(w^{(t)}, g_w^{(t)})$
  - 10:   **end for**
  - 11: **end for**
  - 12: **# Second Step: Search**
  - 13: **for**  $t \leftarrow 1$  to  $T_2$  **do**
  - 14:   Get a batch of data  $X_1$  from  $\chi_1$
  - 15:    $g_w^{(t)} = \nabla_w d(G(X_1, \alpha, \beta, \gamma), G_0(X_1))$
  - 16:    $w^{(t+1)} = \text{update}(w^{(t)}, g_w^{(t)})$
  - 17:   Get a batch of data  $X_2$  from  $\chi_2$
  - 18:    $g_\alpha^{(t)} = \nabla_\alpha d(G(X_2, \alpha, \beta, \gamma), G_0(X_2)) + \lambda \omega_1 \nabla_\alpha F(\alpha | \beta, \gamma)$
  - 19:    $g_\beta^{(t)} = \nabla_\beta d(G(X_2, \alpha, \beta, \gamma), G_0(X_2)) + \lambda \omega_1 \nabla_\beta F(\beta | \alpha, \gamma)$
  - 20:    $g_\gamma^{(t)} = \nabla_\gamma d(G(X_2, \alpha, \beta, \gamma), G_0(X_2)) + \lambda \omega_2 \nabla_\gamma F(\gamma | \alpha, \beta)$
  - 21:    $\alpha^{(t+1)} = \text{update}(\alpha^{(t)}, g_\alpha^{(t)})$
  - 22:    $\beta^{(t+1)} = \text{update}(\beta^{(t)}, g_\beta^{(t)})$
  - 23:    $\gamma^{(t+1)} = \text{update}(\gamma^{(t)}, g_\gamma^{(t)})$
  - 24: **end for**
  - 25: **# Third Step: Train from scratch**
  - 26: Derive the searched architecture  $G^*$  with maximal  $\{\alpha, \beta, \gamma\}$  for each layer and re-initialize weight  $w$ .
  - 27: **for**  $t \leftarrow 1$  to  $T_3$  **do**
  - 28:   Get a batch of data  $X$  from  $\chi$
  - 29:    $g_w^{(t)} = \nabla_w d(G^*(X), G_0(X))$
  - 30:    $w^{(t+1)} = \text{update}(w^{(t)}, g_w^{(t)})$
  - 31: **end for**
- 

parameters  $\gamma$ , we follow [7] to employ a sampling-based strategy. Especially at each step of optimization, we sample only one expansion ratio based on  $\gamma$  and train the model with the selected sub-kernel. Here, Gumbel-softmax [11] is introduced to approximate the sampling process. Thanks to the differentiable Gumbel-softmax, the ratio parameters  $\gamma$  can therefore be optimized in a differentiable framework.

## 4.2. Proxy Task and Optimization

For our trilevel NAS task, instead of training the model from scratch, we leverage the knowledge from pre-trained state-of-the-art image super-resolution models via knowledge distillation [7]. Concretely, we take a pre-trained ES-

RGAN generator as our teacher model, and therefore, the proxy task in the search phase aims to search for a model  $G$  by minimizing the knowledge distillation distance  $d$  between the output from the model  $G$ , and that from the teacher model  $G_0$ . Besides, for the image SR task, an efficient model is always favorable, so we consider involving the model efficiency term  $H$  in our target. Thus, the training objective of the proposed TrilevelNAS is formulated by

$$\min_{G, \alpha, \beta, \gamma} \frac{1}{N} \sum_{i=0}^N d(G(x_i; \alpha, \beta, \gamma), G_0(x_i)) + \lambda_f H(G; \alpha, \beta, \gamma) \quad (5)$$

Here  $\alpha, \beta, \gamma$  are the parameters for the continuous relaxation of the trilevel architecture search space,  $d(G, G_0)$  is a distance for the image SR task, and  $H$  is the computational budget based constraint on the searched architecture. Following [7], we calculate  $d(G, G_0)$  with a combination of content loss  $L_c$  (avoid color shift), perceptual loss  $L_p$  (preserve visual and semantic details), and employ the model FLOPS as a measure of model efficiency.

The suggested continuous relaxation enables us to optimize the network parameters of  $G$ , and all the supernet architecture weights  $\alpha, \beta, \gamma$ . As the number of architecture parameters is much smaller than that of the network parameters, optimizing them jointly on one single training set is likely to overfit. Thus, we alternatively optimize the network weights and architecture parameters under the bi-level optimization framework following differentiable NAS methods. Specially, we separate the dataset into a train set and validation set, where the network weights and architecture parameters are optimized on these two separate sets of data, respectively. Further, since the converged architecture and finally selected architecture is close due to sparsestmax-based supernet relaxation, we go for the new NAS training scheme (*i.e.*, training from search) instead of the conventional training scheme (*i.e.*, training from scratch). Our proposed TrilevelNAS approach is outlined in Algorithm (1).

## 5. Experiments

We evaluate our Trilevel Neural Architecture Search (TrilevelNAS) on PSNR-oriented and visualization-oriented single image super-resolution tasks. For that, we performed search and training on DIV2K and Flickr2K datasets [28]. Further, we evaluated the searched architectures on popular benchmarks, including Set5 [1], Set14 [31], and DIV2K valid set. We use the PSNR as a quantitative metric to measure visual quality. Besides, we report the model size and FLOPS as quantitative metrics for model efficiency, where the FLOPS are calculated when processing a  $256 \times 256$  image. Notably, we implement the Network-Level search with two types of backbone design: (a) **TrilevelNAS-A** Similar to AGD [7], we search for a flexible path of 5 searchable RiR blocks and 2 upsampling

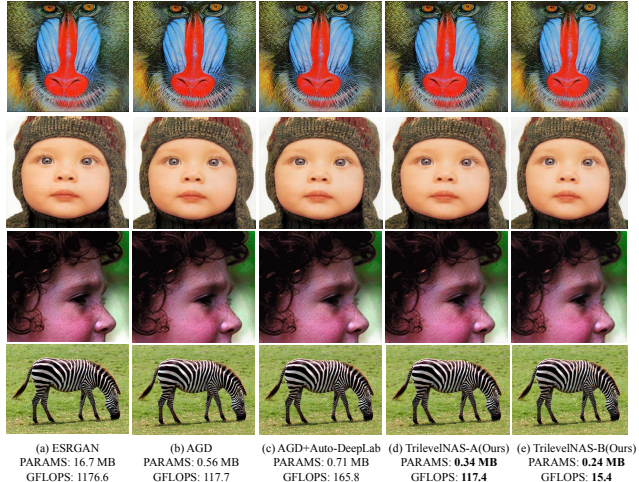


Figure 3: Visualization results of different SR models on Set5 and Set14. It can be observed that TrilevelNAS-B achieves comparable visual quality with very light model.

blocks; (b) **TrilevelNAS-B** For a more efficient SR model, in this backbone, we replace the 2 upsampling layers with a single PixelShuffle block, and search for the path of 5 RiR blocks and 2 convolution layers.

### 5.1. Training Details

In differentiable NAS frameworks, optimization procedure generally consists of three steps: *search*, *model discretization* and *train from scratch*. In contrast, we propose a *Train from Search* framework without the need for a discretization step. Our train from search strategy helps to reduce the model discrepancy between supernet and the discretized stand-alone architecture. Additionally, the progressive sparsity property of sparsestmax encourages the supernet to converge to a sparse network.

- **Search:** Following AGD [7], we split the search process into two phases: the pre-train phase and the search phase. As a warm-up step in the pre-train phase, we use half of the training data to update the network weights for 100 epochs with an only content loss  $L_c$ . After the pre-train phase, we alternatively update the network weights and architecture weights for 100 epochs on two equally split training data. For the PSNR-oriented model search, we only optimize with the content loss  $L_c$ , and for visualization-oriented model search, we finetune with the perceptual loss for a better visual quality. Ultimately, the supernet converges to a single dominant path, where each searchable block has a single operation contribution.
- **Train from Search:** After the entire search process, we do not need a model discretization step with a completely converged supernet. Therefore, we can inherit the pre-trained network weights from the search stage as a good network initialization and continue to train the converged architecture. Following the same training process in AGD [7], for the PSNR-oriented SR model, we train

Method	Path	Params (M)	GFLOPS (256×256)	PSNR		Type
				Set5	Set14	
ESRGAN [30]	-	16.70	1176.6	30.44	26.28	Manual
ESRGAN-prune [16]	-	1.6	113.1	28.07	25.21	Manual
SRGAN [15]	-	1.52	166.7	29.40	26.02	Manual
AGD [7] <sup>†</sup>	-	0.56	117.7	30.36	27.21	Bilevel NAS
AGD-AutoDeepLab	[0,0,0,1,0,0,1]	0.71	165.8	30.48	27.23	Trilevel NAS
TrilevelNAS-A	[0,0,0,1,0,1]	<b>0.34</b>	117.4	30.34	27.29	Trilevel NAS
TrilevelNAS-B	[0,0,0]	<b>0.24</b>	<b>15.4</b>	29.80	27.06	Trilevel NAS

Table 1: Quantitative results of visualization-oriented SR models with scaling factor 4. As for the listed Path results, we use ‘0’ to indicate a *RiR* block and ‘1’ is a *Upsampling* block/*Conv* layer in TrilevelNAS-A/TrilevelNAS-B respectively. † Reproduced AGD with official setup and implementation.

Method	Path	Params (M)	GFLOPS 256×256	PSNR		Type
				Set5	Set14	
ESRGAN [30]	-	16.70	1176.6	32.70	28.95	Manual
HNAS*	Up: 9 <sup>th</sup> layer	1.69	330.7	31.94	28.41	BilevelNAS
AGD [7] <sup>‡</sup>	-	0.90	140.2	31.85	28.40	Bilevel NAS
AGD-AutoDeepLab <sup>†</sup>	[0,0,0,1,0,0,1]	0.71	165.8	31.83	28.38	TrilevelNAS
TrilevelNAS-B	[0, 0, 0, 0, 0, 1]	<b>0.51</b>	<b>33.3</b>	31.62	28.26	Trilevel NAS

Table 2: Quantitative results of PSNR-oriented SR models with scaling factor 4. As for the listed Path results, we use ‘0’ to indicate a *RiR* block and ‘1’ is a *UpConv* layer. Here, the following symbols indicates \* Reproduced HNAS for PSNR-oriented ×4 SR tasks, ‡ Reproduced with AGD official setup and implementation, † Transferred from the visualization-oriented model, respectively.

with only the content loss  $L_c$  for 900 epochs. For the visualization-oriented SR model, we continue to finetune for 1800 epochs with perceptual loss  $L_p$ .<sup>1</sup>

## 5.2. Visualization-oriented SR Model Search

Adopting visualization-oriented ESRGAN [30] model as the teacher model, we apply the TrilevelNAS to search for a visualization-oriented SR model. We compare our method to state-of-art SR GAN models (ESRGAN [30], a pruned ESRGAN baseline [16] and SRGAN [15]) and NAS based visualization-oriented SR model (AGD [7]). Note that we reproduce the AGD search and training results with their official code and default experiment setup. Besides, compared to our Tree-supernet-based Trilevel NAS, we apply the Trellis-supernet design of AutoDeepLab to AGD backbone to implement Trilevel NAS for image SR task.

Table 1 show the statistical comparison of our approach against other competing methods. We additionally report the derived network path (‘0’ in path indicates the *RiR* block; In TrilevelNAS-A, ‘1’ represents an upsampling layer; In TrilevelNAS-B, ‘1’ is a convolution layer). Compared to the AutoDeepLab-based Trilevel NAS (AGD+AutoDeepLab), our TrellisNAS can prune *RiR* blocks or convolution layers, which significantly reduce model complexity. Without a significant change in performance, TrilevelNAS-A prune one redundant *RiR*

<sup>1</sup>For more detailed experiment setups of search and training stages, please refer to our supplementary material.

block and derives a much lighter model with 0.34MB model size. Even with smaller model size, our model still has a comparable FLOPS against AGD. We notice that most of FLOPS consumption come from the blocks operating on high-dimension feature maps. Therefore, when searching for a flexible position of upsampling, if the upsampling appears at an early stage of the network, it is likely to have a dramatic increase in FLOPs consumption. Remarkably, our new backbone (TrilevelNAS-B) has the potential to search for a flexible network-level path with both small model size and light GFLOPs. Compared to original AGD and Trilevel-A, the FLOPs consumption of TrilevelNAS-B is reduced by 4×. We additionally compare the visual qualities of various SR models in Fig 3, and we can see that our TrilevelNAS can derive more efficient SR models without performance loss in visual quality.

## 5.3. PSNR-oriented SR Model Search

We additionally implemented the PSNR-oriented SR model search on DIV2K and Flickr2K datasets and used the PSNR-oriented ESRGAN model as our teacher model. In previous experiments, we have observed a clear FLOPs advantage of our new backbone (Trilevel-B) over the original backbone (Trilevel-A). In this section, we focus on the Trilevel search on our new backbone and aim for a more efficient SR model. We compare our derived model against our competitors in Table 2. With comparable performance, the derived PSNR-oriented SR model on the new back-

Method	Params (M)	GFLOPS	PSNR [Val]	Extra Data	Ground Truth
NJU_MCG	0.43	27.10	29.04	✓	✓
AiriA.CG	0.687	44.98	29.00	✓	✓
HNAS [12]	1.69	330.74	28.86	×	×
AGD [7]	0.45	110.9	28.66	×	×
AGD-AutoDeepLab	0.71	165.8	28.83	×	×
TrilevelNAS-B	<b>0.27</b>	<b>17.33</b>	28.52	×	×

Table 3: Quantitative results on AIM 2020 Challenge [33]

$\lambda$	Path	Params (M)	GFLOPS	PSNR	
				Set5	Set14
0	[0,0,1,0,0,0,1]	0.58	184.08	30.32	27.21
0.01	[0,0,1,0,0,1]	0.52	169.69	30.34	27.20
0.1	[0,0,0,1,0,1]	0.34	117.39	30.34	27.29

Table 4: Quantitative results of visualization-oriented SR models with scaling factor 4 for different ordering constraint strengths. As for the listed Path results, we use ‘0’ to indicate a *RiR* block and ‘1’ is a *UpConv* layer.

Method	Path	Params (M)	GFLOPS	PSNR	
				Set5	Set14
Softmax	[0,0,1,0,1]	0.47	154.80	30.34	27.28
Sparsestmax	[0,0,0,1,0,1]	<b>0.34</b>	<b>117.39</b>	30.34	27.29

Table 5: Quantitative results comparison of visualization-oriented SR models searched using softmax and sparsestmax supernet.

bone prunes a convolution layer and is better in terms of the FLOPs than all other competitors. Further, we compared our model with the winner and runner-up of the recent efficient image super-resolution challenge [33]. Following the challenge setup, we train and validate our model with 800 DIV2K training images and 100 valid images respectively<sup>2</sup>. In Table 3, we present the quantitative results of our method with competing methods, which include challenge winner (NJU\_MCG), runner-up (AiriA.CG), and NAS-based SR models. It can be inferred from the statistics that our method, despite being significantly lighter, gives PSNR value, which is close to competing approaches, and the difference is marginal. Note that, in addition to the challenge methods (i.e., NJU\_MCG and AiriA.CG), all the rest methods do not use the extra data and the ground truth high-resolution images for strong supervision. Instead, these methods just use a teacher model for knowledge distillation. Specially, we follow [7] to adopt the ‘pseudo ground truth’ from a pretrained teacher model for the supervision. This suits the real-world setup more, as the ground-truth high-resolution images are usually not available. Despite this, the PSNR score of our TrilevelNAS is only marginally worse than the challenge winner and runner-up methods.

#### 5.4. Ablation Study

We conducted a few ablation studies to understand better the importance of our proposed ordered Sparsestmax and how it compares against the softmax. Additionally, we

<sup>2</sup>Please refer to supplementary materials for more training details

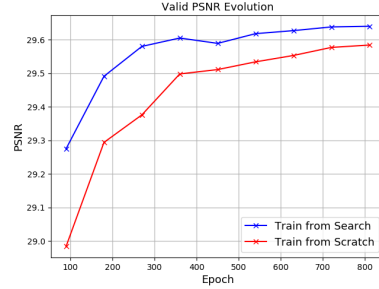


Figure 4: Valid PSNR evolution of *Train from Search* and *Train from Scratch*.

study the effects of training under two different strategies i.e., train from scratch and train from search.

**(a) Sorted Sparsestmax:** For its study, we employ a novel sorted sparsestmax combination of intermediate feature maps to encourage a shallow and efficient SR model without much loss in performance. As formulated in Eq. 3, the ordering constraint factor  $\lambda$  plays a trade-off of the major constraint and ordering constraint, and a large ordering constraint tends to enforce a shallow network. Here, we set  $\lambda$  as 0, 0.01, 0.1, respectively, and study the effects of different ordering constraint strengths on path pruning and the network ability for visualization-oriented SR tasks. Table 4 show the derived paths and the corresponding model performance. We see that without a weight ordering constraint ( $\lambda = 0$ ), the TrellisNAS prefers a full network path with 5 *RiR* blocks and 2 upsampling blocks. When we impose ordering constraint with  $\lambda=0.01, 0.1$ , the tail *RiR* block is seen to be pruned, which yields more efficient SR models with small model size and FLOPs without loss in performance.

**(b) Softmax vs. Sparsestmax:** To perform this ablation study, instead of applying softmax combinations of candidates, we propose using sparsestmax combination. With the same ordering constraint strategy for feature maps weights, we study the supernet optimization with softmax and sparsestmax combination, respectively. From Table 5, we can notice that with weight ordering constraint, softmax and sparsestmax can prune one or two *RiR* blocks and have comparable performance in PSNR. In contrast, sparsestmax converges to a more efficient model with a smaller model size and GFLOPs consumption.

**(c) Train from Search vs. Train from Scratch:** Lastly, we study the effect of inheriting weights from the search phase. Fig. 4 shows the valid PSNR evolution of training from search and training from scratch, respectively, and we can observe a clear advantage of inheriting weights from the search phase. With the training from search strategy, we can converge to a better PSNR performance using fewer epochs.

## 6. Conclusion and Future Work

In this paper, we introduced Trilevel NAS for a single image super-resolution task. Our work demonstrates the possibility of exploring the valid search space at network-level,



cell-level, and the kernel-level. By introducing the proposed tri-level search space’s continuous relaxation, we build a hierarchical mixture of the network path. Instead of relying on the trellis-like network modeling, we show the utility of a tree-like supernet modeling with sparsestmax activation to the NAS framework. The architecture obtained after our proposed optimization show that, despite being much lighter, it can perform as good as the best available algorithms. For future work, we plan to apply the proposed sorted sparsestmax to further relax the kernel-level search space to achieve more effective SR (e.g., higher PSNR and better perceptual quality) with searched architectures as light as possible.

## Acknowledgements

This work was supported by the ETH Zürich Fund (OK), a Huawei (Moscow) project, an Amazon AWS grant, and an Nvidia GPU grant. Suryansh Kumar’s work is supported by “ETH Zürich Foundation and Google, Project Number: 2019-HE-323 (2)” for bringing together best academic and industrial research.

## References

- [1] Marco Bevilacqua, Aline Roumy, Christine Guillemot, and Marie Line Alberi-Morel. Low-complexity single-image super-resolution based on nonnegative neighbor embedding, 2012. [2](#), [6](#)
- [2] Han Cai, Ligeng Zhu, and Song Han. Proxylessnas: Direct neural architecture search on target task and hardware. *CoRR*, abs/1812.00332, 2018. [2](#)
- [3] Xin Chen, Lingxi Xie, Jun Wu, and Qi Tian. Progressive darts: Bridging the optimization gap for nas in the wild. 2020. [2](#)
- [4] Xiangxiang Chu, Tianbao Zhou, Bo Zhang, and Jixiang Li. Fair darts: Eliminating unfair advantages in differentiable architecture search. 2020. [1](#), [2](#)
- [5] Tao Dai, Jianrui Cai, Yongbing Zhang, Shu-Tao Xia, and Lei Zhang. Second-order attention network for single image super-resolution. In *Proceedings of the IEEE conference on computer vision and pattern recognition*, pages 11065–11074, 2019. [1](#)
- [6] Chao Dong, Chen Change Loy, Kaiming He, and Xiaoou Tang. Image super-resolution using deep convolutional networks. *CoRR*, abs/1501.00092, 2015. [1](#)
- [7] Yonggan Fu, Wuyang Chen, Haotao Wang, Haoran Li, Yingyan Lin, and Zhangyang Wang. Autogandistiller: Searching to compress generative adversarial networks. 2020. [1](#), [2](#), [3](#), [4](#), [5](#), [6](#), [7](#), [8](#)
- [8] Yonggan Fu, Wuyang Chen, Haotao Wang, Haoran Li, Yingyan Lin, and Zhangyang Wang. Autogandistiller: Searching to compress generative adversarial networks. *arXiv preprint arXiv:2006.08198*, 2020. [11](#)
- [9] Chen Gao, Yunpeng Chen, Si Liu, Zhenxiong Tan, and Shuicheng Yan. Adversarialnas: Adversarial neural architecture search for gans. 2020. [2](#)
- [10] Xinyu Gong, Shiyu Chang, Yifan Jiang, and Zhangyang Wang. Autogan: Neural architecture search for generative adversarial networks. 2019. [2](#)
- [11] E.J. Gumbel. *Statistical Theory of Extreme Values and Some Practical Applications: A Series of Lectures*. Applied mathematics series. U.S. Government Printing Office, 1954. [5](#)
- [12] Yong Guo, Yongsheng Luo, Zhenhao He, Jin Huang, and Jian Chen. Hierarchical neural architecture search for single image super-resolution. *IEEE Signal Processing Letters*, 27:1255–1259, 2020. [1](#), [3](#), [8](#)
- [13] Jiwon Kim, Jung Kwon Lee, and Kyoung Mu Lee. Deeply-recursive convolutional network for image super-resolution. *CoRR*, abs/1511.04491, 2015. [1](#)
- [14] Christian Ledig, Lucas Theis, Ferenc Huszár, Jose Caballero, Andrew Cunningham, Alejandro Acosta, Andrew Aitken, Alykhan Tejani, Johannes Totz, Zehan Wang, et al. Photo-realistic single image super-resolution using a generative adversarial network. In *Proceedings of the IEEE conference on computer vision and pattern recognition*, pages 4681–4690, 2017. [3](#)
- [15] Christian Ledig, Lucas Theis, Ferenc Huszar, Jose Caballero, Andrew Cunningham, Alejandro Acosta, Andrew Aitken, Alykhan Tejani, Johannes Totz, Zehan Wang, and Wenzhe Shi. Photo-realistic single image super-resolution using a generative adversarial network. 2017. [1](#), [7](#)
- [16] Hao Li, Asim Kadav, Igor Durdanovic, Hanan Samet, and Hans Peter Graf. Pruning filters for efficient convnets. *CoRR*, abs/1608.08710, 2016. [7](#)
- [17] M. Li, J. Lin, Y. Ding, Z. Liu, J. Y. Zhu, and S. Han. Gan compression: Efficient architectures for interactive conditional gans. In *2020 IEEE/CVF Conference on Computer Vision and Pattern Recognition (CVPR)*, pages 5283–5293, 2020. [1](#)
- [18] Zhen Li, Jinglei Yang, Zheng Liu, Xiaomin Yang, Gwanggil Jeon, and Wei Wu. Feedback network for image super-resolution. *CoRR*, abs/1903.09814, 2019. [1](#)
- [19] Chenxi Liu, Liang-Chieh Chen, Florian Schroff, Hartwig Adam, Wei Hua, Alan L. Yuille, and Li Fei-Fei. Auto-deeplab: Hierarchical neural architecture search for semantic image segmentation. *CoRR*, abs/1901.02985, 2019. [1](#), [2](#), [3](#), [4](#), [11](#)
- [20] Hanxiao Liu, Karen Simonyan, and Yiming Yang. Darts: Differentiable architecture search. *arXiv preprint arXiv:1806.09055*, 2018. [1](#), [2](#), [3](#), [4](#)

- [21] André F. T. Martins and Ramón Fernandez Astudillo. From softmax to sparsemax: A sparse model of attention and multi-label classification. *CoRR*, abs/1602.02068, 2016. 5
- [22] Vlad Niculae and Mathieu Blondel. A regularized framework for sparse and structured neural attention. In *Advances in neural information processing systems*, pages 3338–3348, 2017. 5
- [23] Esteban Real, Alok Aggarwal, Yanping Huang, and Quoc V Le. Regularized evolution for image classifier architecture search. 2019. 2
- [24] Esteban Real, Sherry Moore, Andrew Selle, Saurabh Saxena, Yutaka Leon Suematsu, Jie Tan, Quoc V Le, and Alexey Kurakin. Large-scale evolution of image classifiers. In *International Conference on Machine Learning*, pages 2902–2911, 2017. 2
- [25] Wenqi Shao, Tianjian Meng, Jingyu Li, Ruimao Zhang, Yudian Li, Xiaogang Wang, and Ping Luo. SSN: learning sparse switchable normalization via sparsestmax. *CoRR*, abs/1903.03793, 2019. 2
- [26] Wenqi Shao, Tianjian Meng, Jingyu Li, Ruimao Zhang, Yudian Li, Xiaogang Wang, and Ping Luo. Ssn: Learning sparse switchable normalization via sparsestmax. 2019. 4, 5, 11
- [27] Dimitrios Stamoulis, Ruizhou Ding, Di Wang, Dimitrios Lymberopoulos, Bodhi Priyantha, Jie Liu, and Diana Marculescu. Single-path nas: Designing hardware-efficient convnets in less than 4 hours. In *Joint European Conference on Machine Learning and Knowledge Discovery in Databases*, pages 481–497. Springer, 2019. 2
- [28] Radu Timofte, Eirikur Agustsson, Luc Van Gool, Ming-Hsuan Yang, and Lei Zhang. Ntire 2017 challenge on single image super-resolution: Methods and results. In *Proceedings of the IEEE conference on computer vision and pattern recognition workshops*, pages 114–125, 2017. 6, 10, 11, 13
- [29] Tong Tong, Gen Li, Xiejie Liu, and Qinquan Gao. Image super-resolution using dense skip connections. pages 4809–4817, 10 2017. 1
- [30] Xintao Wang, Ke Yu, Shixiang Wu, Jinjin Gu, Yihao Liu, Chao Dong, Chen Change Loy, Yu Qiao, and Xiaoou Tang. ESRGAN: enhanced super-resolution generative adversarial networks. *CoRR*, abs/1809.00219, 2018. 1, 7
- [31] Roman Zeyde, Michael Elad, and Matan Protter. On single image scale-up using sparse-representations. In *International conference on curves and surfaces*, pages 711–730. Springer, 2010. 2, 6
- [32] Haokui Zhang, Ying Li, Hao Chen, and Chunhua Shen. Memory-efficient hierarchical neural architecture search for image denoising. 2020. 2
- [33] Kai Zhang, Martin Danelljan, Yawei Li, Radu Timofte, Jie Liu, Jie Tang, Gangshan Wu, Yu Zhu, Xiangyu He, Wenjie Xu, et al. Aim 2020 challenge on efficient super-resolution: Methods and results. *arXiv preprint arXiv:2009.06943*, 2020. 2, 3, 8, 13
- [34] Barret Zoph and Quoc V Le. Neural architecture search with reinforcement learning. *ICLR*, 2017. 2
- [35] Barret Zoph, Vijay Vasudevan, Jonathon Shlens, and Quoc V Le. Learning transferable architectures for scalable image recognition. In *Proceedings of the IEEE conference on computer vision and pattern recognition*, pages 8697–8710, 2018. 2

## Appendix

### A. Implementation Details

In this section, we describe the implementation details of our trilevel NAS algorithm for the SR task. The search strategy using visualization and the PSNR-oriented teacher model is discussed, followed by the training strategy. The code is developed with Python 3.6 and Pytorch 1.3.1. The complete search process takes 8 GPU days on single NVIDIA Tesla V100 (16GB RAM) and the training of a PSNR-oriented and visualization-oriented SR model take 0.5 and 1.5 GPU days respectively.

#### A.1. Search

We implement our search phase using DIV2K and Flickr2K dataset [28].

**(a) Visualization-oriented:** Here, we took the visualization-oriented ESRGAN model as a teacher model for the SR model search task. Subsequently, we perform the search task in two phase: (a) *Pretrain*: using half of the training data, we optimize the content loss  $L_c$  and train the supernet weights without updating architecture parameters. We train for 100 epochs using Adam optimizer, and at each optimization step, 3 patches of size  $32 \times 32$  are randomly cropped. For architecture parameters, we use a constant learning rate  $3 \times 10^{-4}$ , and for network weights, we set the initial learning rate as  $1 \times 10^{-4}$ , decayed by 0.5 at 25<sup>th</sup>, 50<sup>th</sup>, 75<sup>th</sup> epoch. (b) *Search*: optimizing content loss  $L_c$  and perceptual loss  $L_p$ , we alternatively update the network weights and architecture weights for 100 epochs on two equally split training data. The optimizer follows the same setting as in the pretrain phase.

**(b) PSNR-oriented:** For this, we took the PSNR-oriented ESRGAN model as teacher model for SR model search and followed the similar procedure *i.e.*, *Pretrain* and *Search*, and however, here we optimize only the content loss  $L_c$  in the two phases.

Method	Path	Params (M)	GFLOPS	PSNR	
				Set5	Set14
BilevelNAS	-	0.52	115.39	30.32	27.22
TrilevelNAS	[0,0,0,1,0,1]	<b>0.34</b>	117.39	30.34	27.29

Table 6: Quantitative results comparison of BilevelNAS (kernel- and cell-level) and TrilevelNAS (kernel-, cell- and network-level).

## A.2. Train

We inherit the weights from supernet and train with DIV2K and Flickr2K datasets [28] in the training phase. Patches of size  $32 \times 32$  are randomly cropped, and the batch size is set to 16.

**Visualization-oriented:** SR model training is conducted in two steps: (a) *Pretrain* by minimizing content loss  $L_c$  for 900 epochs. Adam optimizer is used with initial learning rate  $1 \times 10^{-4}$  and learning rate decays by 0.5 at 225<sup>th</sup>, 450<sup>th</sup>, 675<sup>th</sup> epoch. (b) *Fine-tune* with perceptual loss  $L_p$  for 1800 epochs. We also train with Adam optimizer with initial learning rate  $1 \times 10^{-4}$ , decayed by 0.5 at 225<sup>th</sup>, 450<sup>th</sup>, 900<sup>th</sup>, 1350<sup>th</sup> epoch.

**PSNR-oriented:** SR model is trained by minimizing the content loss  $L_c$  for 900 epochs, and the optimizer follows the same setting as the pretrain phase in visualization-oriented model training. Note that, for the challenge setup, we only train our proposed model with DIV2K (without using extra data), and merely use a teacher for data distillation instead of using the ground truth for strong supervision, which might lead to marginally inferior performance. We first crop LR images in DIV2K into sub-images of size  $120 \times 120$ . We use Adam to train for 300 epochs, where the learning rate decays by 0.5 at 75<sup>th</sup>, 150<sup>th</sup>, 225<sup>th</sup> epoch.

## B. Ablation Study

We performed the following ablation study the advantage of performing trilevel NAS as compared to bilevel NAS [8] [19] using the sparsestmax continuous relaxation [26]. This experimental setup shall help understand the utility of exhaustive search to obtain the light-weight model without sacrificing much on the performance.

**Bilevel vs. Trilevel:** To show the necessity and advantage of introducing our network-level search in addition to cell-level and kernel-level search, we compare the BilevelNAS, which has a fixed network-level design (*i.e.*, path: [0, 0, 0, 0, 0, 1, 1]) with our TrilevelNAS. For BilevelNAS, we use AGD [8], and for a fair comparison, we replace the original softmax combination in AGD with sparsestmax combination. From Table 6, we can conclude that the additional network-level search in TrilevelNAS enables us to derive a lighter model with comparable performance. It can be inferred from the Table 6 statistics that the number of parameters in our approach is significantly smaller as compared to BilevelNAS, whereas the PSNR value is slightly better with comparable GFLOPS on Set5 and Set14.

## C. Architecture Details

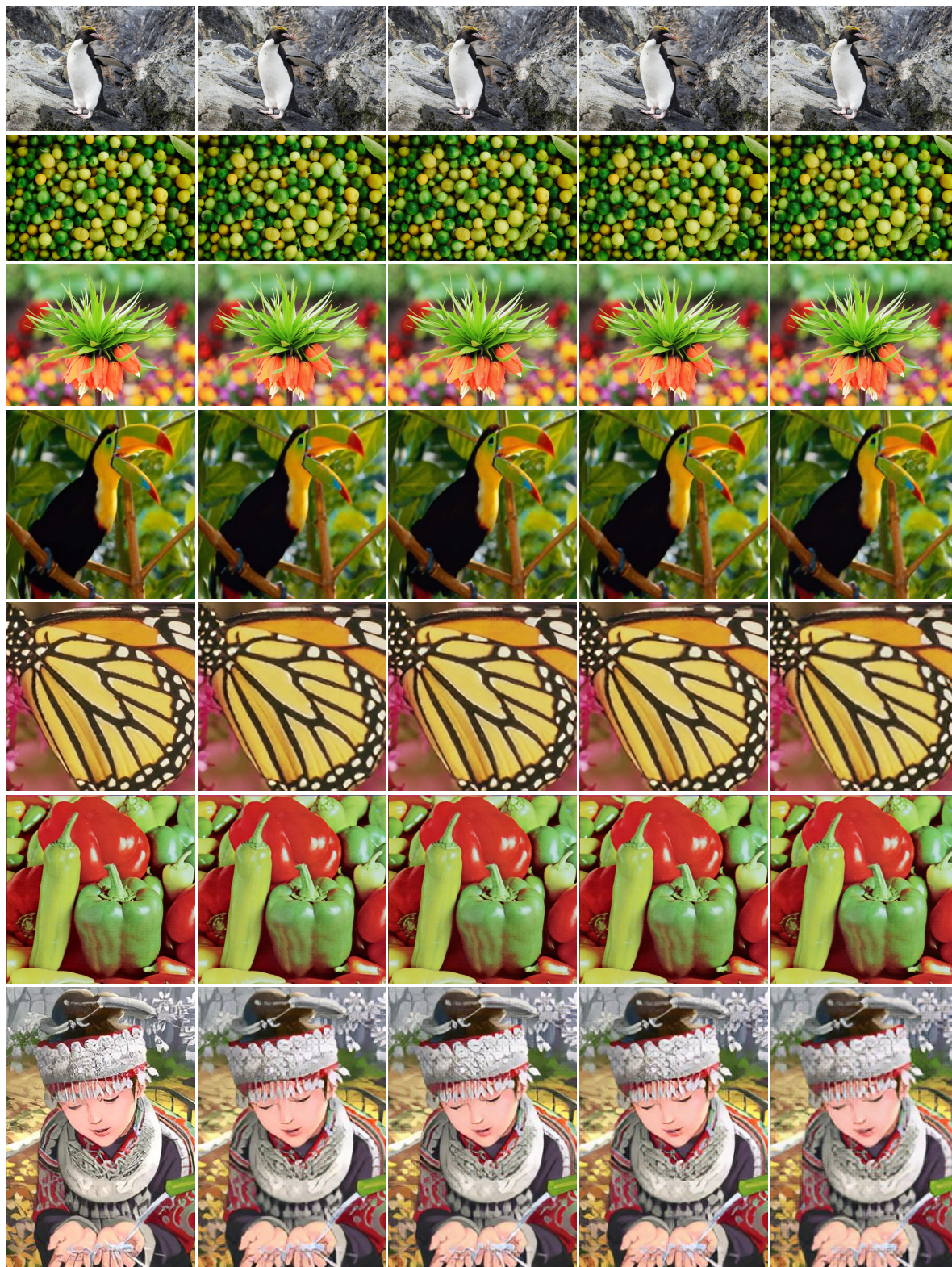
Table 7-10 present our derived network-level (path), cell-level (5 searchable operations in each RiR block) and kernel-level (output channel number) architectures. Table 7-8 show the SR architecture model obtained using visualization-oriented search strategy on DIV2K and Flickr2K dataset, whereas, Table 9-10 provide the SR architecture obtained using PSNR-oriented search strategy.

The obtained network-level path is shown in first row of the respective table. The entry ‘0’ and ‘1’ in the path-index row-vector indicates RiR block and upsampling/convolution layer respectively. In addition, we lists the cell-level structures (*i.e.*, the selection of operations in OP1-OP5 in each RiR block) and the kernel-level structures (*i.e.*, the selection of output channels from the full 64 channels) in Table 9-10. For each OP, the format ( $A, B$ ) indicates selecting the operation  $A$  with its kernel width being  $B$ . Regarding the types of different OPs, DwsBlock, ResBlock, Conv symbolises depthwise convolution block, residual block and convolution block respectively.

## D. More Visualization Results

Figure 5 show the visual comparison of our approach against other competing methods. The last two columns in the figure show the results obtained using our approach with TrilevelNAS-A and TrilevelNAS-B search strategy, respectively. Clearly, our method supplies a significantly lighter model and provides a super-resolved image that is perceptually as good as, if not better, than other approach results.





(a) ESRGAN	(b) AGD	(c) AGD+Auto-DeepLab	(d) TrilevelNAS-A(Ours)	(e) TrilevelNAS-B(Ours)
PARAMS: 16.7 MB	PARAMS: 0.56 MB	PARAMS: 0.71 MB	PARAMS: <b>0.34 MB</b>	PARAMS: <b>0.24 MB</b>
GFLOPS: 1176.6	GFLOPS: 117.7	GFLOPS: 165.8	GFLOPS: <b>117.4</b>	GFLOPS: <b>15.4</b>

Figure 5: Visualization results of different SR models on Set5, Set14 and DIV2K valid set. Our TrilevelNAS-A and TrilevelNAS-B achieve comparable visual quality with very light model.



Path	[0, 0, 0, 1, 0, 1]				
RiR Block ID	OP1	OP2	OP3	OP4	OP5
0	(Conv $1 \times 1$ , 64)	(Conv $3 \times 3$ , 24)	(Conv $1 \times 1$ , 24)	(Conv $1 \times 1$ , 24)	(Conv $3 \times 3$ , 64)
1	(DwsBlock, 32)	(DwsBlock, 32)	(DwsBlock, 64)	(Conv $3 \times 3$ , 24)	(ResBlock, 64)
2	(Conv $1 \times 1$ , 64)	(Conv $1 \times 1$ , 64)	(Conv $3 \times 3$ , 40)	(Conv $1 \times 1$ , 32)	(DwsBlock, 64)
3	(Conv $3 \times 3$ , 24)	(Conv $3 \times 3$ , 64)	(Conv $1 \times 1$ , 32)	(Conv $3 \times 3$ , 32)	(Conv $3 \times 3$ , 64)

Table 7: Visualization-oriented SR model architecture searched on DIV2K and Flickr2K dataset [28] with original AGD backbone (TrilevelNAS-A). We present the network-level architecture (i.e., path of stacking RiR blocks and upsampling layers), the cell-level structures (i.e., the selection of operations in OP1-OP5 in each RiR block) and the kernel-level structures (i.e., the selection of output channels from the full 64 channels). In the path, '0' indicates a RiR block and the '1' indicates an upsampling layer. For each OP, the format  $(A, B)$  indicates selecting the operation  $A$  with its kernel width being  $B$ .

Path	[0, 0, 0]				
RiR Block ID	OP1	OP2	OP3	OP4	OP5
0	(DwsBlock, 32)	(Conv $1 \times 1$ , 32)	(DwsBlock, 24)	(DwsBlock, 40)	(DwsBlock, 64)
1	(DwsBlock, 24)	(Conv $1 \times 1$ , 56)	(Conv $3 \times 3$ , 24)	(DwsBlock, 24)	(Conv $3 \times 3$ , 64)
2	(ResBlock, 64)	(Conv $1 \times 1$ , 24)	(Conv $1 \times 1$ , 24)	(Conv $1 \times 1$ , 24)	(Conv $1 \times 1$ , 64)

Table 8: Visualization-oriented SR model architecture searched on DIV2K and Flickr2K dataset [28] with our proposed new backbone (TrilevelNAS-B). We present the network-level architecture (i.e., path of stacking RiR blocks and convolutional layers), the cell-level structures (i.e., the selection of operations in OP1-OP5 in each RiR block) and the kernel-level structures (i.e., the selection of output channels from the full 64 channels). In the path, '0' indicates a RiR block and the '1' indicates a convolutional layer. For each OP, the format  $(A, B)$  indicates selecting the operation  $A$  with its kernel width being  $B$ .

Path	[0, 0, 0, 0, 0, 1]				
RiR Block ID	OP1	OP2	OP3	OP4	OP5
0	(Conv $1 \times 1$ , 32)	(Conv $1 \times 1$ , 24)	(DwsBlock, 64)	(DwsBlock, 24)	(Conv $1 \times 1$ , 64)
1	(DwsBlock, 32)	(ResBlock, 40)	(DwsBlock, 56)	(Conv $3 \times 3$ , 40)	(Conv $3 \times 3$ , 64)
2	(Conv $3 \times 3$ , 64)	(Conv $1 \times 1$ , 64)	(Conv $3 \times 3$ , 24)	(Conv $1 \times 1$ , 32)	(DwsBlock, 64)
3	(DwsBlock, 64)	(DwsBlock, 56)	(Conv $3 \times 3$ , 24)	(Conv $3 \times 3$ , 24)	(DwsBlock, 64)
4	(DwsBlock, 32)	(Conv $3 \times 3$ , 64)	(Conv $3 \times 3$ , 64)	(Conv $3 \times 3$ , 24)	(Conv $3 \times 3$ , 64)

Table 9: PSNR-oriented SR model architecture searched on DIV2K and Flickr2K [28] with our new backbone (TrilevelNAS-B). We present the network-level architecture (i.e., path of stacking RiR blocks and convolutional layers), the cell-level structures (i.e., the selection of operations in OP1-OP5 in each RiR block) and the kernel-level structures (i.e., the selection of output channels from the full 64 channels). In the path, '0' indicates a RiR block and the '1' indicates a convolutional layer. For each OP, the format  $(A, B)$  indicates selecting the operation  $A$  with its kernel width being  $B$ .

Path	[0, 0, 1, 1]				
RiR Block ID	OP1	OP2	OP3	OP4	OP5
0	(Conv $1 \times 1$ , 40)	(Conv $1 \times 1$ , 24)	(Conv $1 \times 1$ , 56)	(ResBlock, 56)	(Conv $1 \times 1$ , 64)
1	(DwsBlock, 64)	(DwsBlock, 56)	(Conv $3 \times 3$ , 32)	(Conv $3 \times 3$ , 24)	(Conv $1 \times 1$ , 64)

Table 10: PSNR-oriented SR model architecture searched on DIV2K and Flickr2K [28] with our proposed TrilevelNAS-B on AIM challenge [33]. We present the network-level structures (i.e., path of stacking RiR blocks and convolutional layers), the cell-level structures (i.e., the selection of operations in OP1-OP5 in each RiR block) and the kernel-level structure (i.e., the selection of output channels from the full 64 channels). In the path, '0' indicates a RiR block and the '1' indicates a convolutional layer. For each OP, the format  $(A, B)$  indicates selecting the operation  $A$  with its kernel width being  $B$ .